The Numerical Analysis of Influence of the Shape of the Anchor Head on the Headed Stud´s Tensile Capacity

Jindřich Fornůsek[1a], Petr Konvalinka[1]

[1]Experimental Center, Faculty of Civil Engineering, CTU in Prague, Czech Republic

[a]jindrich.fornusek@fsv.cvut.cz

Keywords: Anchorage, Capacity, Concrete, Headed Studs, Head Shape, Tension

Abstract. This paper deals with the numerical analysis of the headed stud´s tensile behavior in dependence on the shape and size of the head. Forty-eight 2D axi-symmetric numerical models were carried out. Three different embedment depths (50, 150 and 450 mm), each with four different angles of the top head surface (0, 20, 40 and 60 degrees) and four different head sizes (d_h/h_{ef} = 0,15; 0,2; 0,3 or 0,4). The concrete behavior was simulated by the Nonlinear Cementitious2 fracture-plastic material model. The results of the analysis showed that the shape (angle) has only the negligible effect on the tensile capacity especially for the small heads. The more significant increase of the capacity was observed within the large head size where the increase of the bearing area due to the different angle is more significant.

Introduction

The anchorage systems for fixing the structural members to concrete are well known for many years. These systems are used very often to transfer the tensile, shear or both loads into the concrete and it was proved by many experimental and numerical researches that these systems are able to transfer these kind of loads into the concrete without connecting to the reinforcement. Two basic groups of anchorage systems can be found: cast-in-place headed studs which are placed into the mould before concrete casting and post-installed anchors (undercut, expansion, adhesive etc.) which are installed into the hardened concrete [1]. There are four basic failure modes of anchorage systems: steel yielding, pulling-out, concrete splitting and concrete cone breakout [2]. This paper is focused on the behavior of the cast-in-place headed studs and it´s cone breakout capacity in dependence on the shape of the head.

There were carried out many experimental and numerical researches that helped to find out reliable formulas for the calculation of cone breakout capacity of anchorage systems. The most of the research work was focused of the anchors with effective embedment depths up to c. 500 mm and with the concrete compressive strength f_{cu} between 20 to 50 MPa[3-6] since these ranges are the most common in current constructions. Based on the previous researches two dominant methods of cone breakout capacity were established: 45-degree Cone Method (45CM) which was developed in the United States in 1970´s [7] and is mainly related to the nuclear structures [8] and Concrete Capacity Design (CCD) which was introduced in early 1990´s [1] and nowadays is adopted by many national standards including the Eurocode [9]. The 45-degree Cone Method is based on the presumption that constant tensile stress which is equaled to $0,96f\sqrt{f_c'}$ acts on the projected area of the failure cone with inclination between the failure surface and concrete surface 45 degrees [10] (Fig. 1a). The equation for calculation of breakout cone capacity F_u of single anchor is:

$$F_{u,45CM} = 0,96\sqrt{f_c'}\,\pi h_{ef}^2\left(1 + {}^{d_h}\!/_{h_{ef}}\right); N \qquad (1)$$

with:

f_c' concrete compressive cylinder strength, (MPa);

d_h diameter of anchor head, (mm);

h_{ef} effective embedment depth , (mm).

The CCD approach idealizes the breakout body of concrete as a pyramid with the base of $3h_{ef}$ by $3h_{ef}$ and the inclination between failure surface and concrete surface is approximately 35 degrees (Fig. 1b) [2]. The equation for calculation of capacity of single anchor is based on widespread observations, large amount of experimental data and fracture mechanics of concrete:

$$F_{u,CCD} = k\sqrt{f_{cu}}\,h_{ef}^{1,5}; N \qquad (2)$$

with:

k is 13,5 for post installed fasteners and 15,5 for cast-in-place headed studs [1];

f_{cu} cubic concrete compressive strength, (MPa);

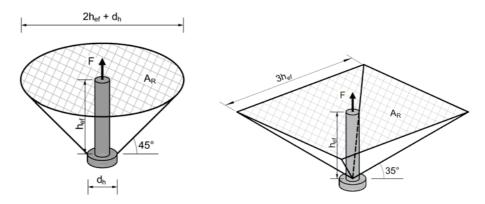h_{ef} effective embedment depth, (mm).

Fig. 1. The idealization of breakout cone by 45CM (a) and pyramid by CCD method (b)

Numerical model

    The 2D axi-symmetric model was created for the simulation of tensile behavior. The geometry of the model is specified in the Fig. 2. The geometry of all models was kept similar, only changes were the parameters stated in the Tab. 1.
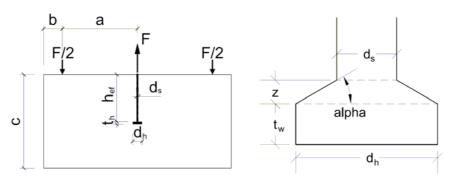

Fig. 2. The scheme of geometry and the detail of the shape of the head

Tab. 1: Geometry of the numerical model

h_{ef}	a	b	c	d_h	α	d_s	t_h
(mm)	(mm)	(mm)	(mm)	(mm)	(deg)	(mm)	(mm)
50	150	50	200	7,5; 10; 15; 20		5	8
150	450	150	600	22,5; 30; 45; 60	0; 20; 40; 60	15	24
450	1350	450	1800	67,5; 90; 135; 180		45	72

The concrete block was divided into the three main parts for the discretization which were connected by the fixed contact. The fixed contact is special Dirichlet type complex boundary condition so called master-slave boundary conditions [11]. The isoparametric plane quadrilateral elements with integration in four points were used for the mesh. The typical mesh is presented in Fig. 3. In the upper area where the crack was predicted the mesh was more fine and concentrated to the location where the steel head of the anchor was connected to the concrete. The head of the anchor was fixed to the concrete block only through the top line, the side and the bottom of the head was not connected to avoid the transfer of shear and tension into the concrete. The mesh was kept similar for all the simulations. The displacement was applied on the top free line of the head in 30 to 60 steps to simulate the progressive loading. The presence of the shank of the anchor was replaced by the nonlinear spring constraint to avoid the concrete pushing into the shank cavity. The vertical constraint was set on the support ring where the reaction F_u was monitored.
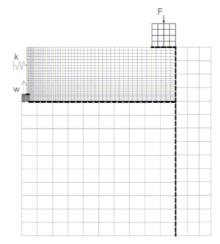

Fig. 3. Mesh of the numerical model (fixed contacts – dashed line)

The Nonlinear Cementitious2 (C2) material model was selected to simulate the concrete block behaviour. The C2 is the fracture-plastic numerical model which combines constitutive models for tensile (fracturing) and compressive (plastic) behaviour. The fracture model is based on the orthotropic smeared cracks and crack band model. It employs Rankine failure criterion, exponential softening and it can be used as rotated or fixed cracks. The hardening/softening plasticity model is based on Menétrey-William failure surface. This model can be used to simulate concrete cracking, crushing under high confinement and crack closure due to crushing in other material directions [11].

The bilinear von Mises material model was set for the steel (anchor head and support ring) with yield strength $f_y = 550$ MPa, elasticity modulus $E_s = 200$ GPa; Poisson´s ratio $v = 0,3$ and hardening modulus $H = 10$ GPa [11] .

Tab. 2 Material parameters of the numerical model

f_{cu}	E^1	f_t^1	G_f^2
(MPa)	(GPa)	(MPa)	(N/m)
30	30,3	2,32	57,9

[1] completed from f_{cu} by equations [12]: $f_t = 0,24 f_{cu}^{2/3}$; $E_c = (6000-15,5 f_{cu}) . \sqrt{f_{cu}}$ (MPa)
[2] completed from f_t by equation [13]: $G_f = 25 f_t$ (N/m)

Results of numerical analysis

The results of numerical analyses are summarized in the Tab. 3. In the Fig. 4 (a – h_{ef} = 50; b – h_{ef} = 150; c – h_{ef} = 450 mm) the peak loads are compared to the peak load of the headed stud with flat bearing area (α = 0 deg). It can be seen that the influence of the angle is stronger with the increasing head size and it is very similar for all embedment depths. For the small heads the change of the capacity was negligible. The increase of the capacity is caused by the increase of the bearing area A_b of the head by the increase of the head diameter and also by the cone shape. The bearing area of the cone shaped head can be calculated by Eq.(3):

$$A_b = \pi \cdot \left(\frac{d_h + d_s}{2} \right) \cdot \sqrt{z^2 + \left(\frac{d_h - d_s}{2} \right)^2} \qquad (3)$$

with:
A_b bearing area of the head (mm^2);
d_h head diameter (mm);
d_s shank diameter (mm);
z height of the frustum cone of the head (mm)

Since the angles change in the step of 20 degrees the bearing area A_b changes also regularly along to the Eq.(3) for all effective embedment depths and head diameters. The ratio between the bearing area where the angle is 0 degrees and the other bearing areas with different angle is: $A_{b,20}$ / $A_{b,0}$ = 1,06; $A_{b,40}$ / $A_{b,0}$ = 1,31; $A_{b,60}$ / $A_{b,0}$ = 2,0. In the Fig. 5 there are compared the peak loads F_u normalized to the ultimate capacity via CCD approach $F_{u,CCD}$. For each effective embedment depth the bearing area A_b is also normalized to the A_b* where d_h/h_{ef} = 0,15 and α = 0 deg. The coefficient of the capacity increase in dependence on the bearing area is also introduced Eq. (4):

$$F_u = \frac{150}{\sqrt{hef}} \cdot A_b^{0,35} \qquad (4)$$

This coefficient is different to the one found in previous research [14] while it was necessary to add the influence of changing bearing area with the angle of the head.
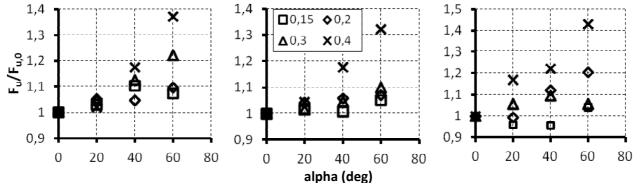

Fig. 4: Diagrams of peak loads (normalized to the $F_{u,0}$ where α = 0 deg); a – h_{ef} = 50, b – h_{ef} = 150 and c – h_{ef} = 450 mm

Tab. 3: Ultimate peak loads and displacements

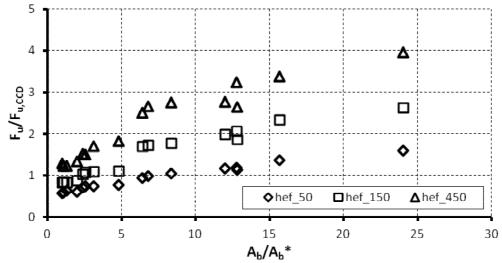| d_h/h_{ef} | α | h_{ef} | | | | | |
| | | 50 | | 150 | | 450 | |
(-)	(deg)	F_u(kN)	w (mm)	F_u(kN)	w (mm)	F_u(kN)	w (mm)
0,15	0	17,3	2,4	131,3	4,1	1058,4	8,2
	20	17,8	2,4	133,4	4,5	1014,4	5,8
	40	19,1	2,2	132,2	5,3	1011,1	7,1
	60	18,6	3,4	138,0	5,8	1101,8	10,9
0,2	0	21,6	1,3	163,1	1,9	1246,3	4,7
	20	22,7	1,6	169,9	2,4	1237,9	4,3
	40	22,6	1,7	172,5	2,9	1397,5	10,1
	60	23,7	2,0	174,4	3,6	1501,5	9,5
0,3	0	28,5	0,5	270,0	2,2	2071,4	6,1
	20	29,9	0,5	273,6	2	2186,9	8,3
	40	32,1	0,6	282,4	2,1	2268,1	7,6
	60	34,8	0,8	296,4	1,8	2183,7	4,2
0,4	0	35,6	0,5	314,9	2,4	2283,1	5,2
	20	36,3	0,5	328,5	2,1	2665,8	6,1
	40	41,8	0,6	370,7	2,3	2788,1	5,4
	60	48,8	0,6	416,7	2,4	3264,0	4,9

Fig. 5: Diagram of normalized peak loads and bearing areas

Conclusion

The numerical analysis of forty-eight models of headed stud with different head size and angle of the top head surface (bearing area) breakout capacity was carried out in this paper. It was found that the angle of the bearing area can positively affect the capacity of the headed stud especially the studs with large heads. The coefficient of the capacity increase was based on the results on the analysis. Nonetheless the most dominant effect on the capacity increase was the head size (diameter) instead of the angle of the top bearing area. There for the influence of the angle of the bearing area can be neglected especially for the studs with relatively small heads.

Acknowledgment

References

[1] W. Fuchs, R. Eligehausen, J. E. Breen, Concrete capacity design (CCD) approach for fastening to concrete, ACI Struct.J., 92, 1, ACI, 1995,.

[2] Comité Euro-International du Béton, Design of Fastenings to Concrete, Thomas Telford Services Ltd., London, 1997,.

[3] J. Ožbolt, R. Eligehausen, G. Periškić, U. Mayer, 3D FE analysis of anchor bolts with large embedment depths, Fracture of Concrete Materials and Structures,Eng.Fract.Mech., 74, 1–2, 2007, pp. 168-178, 0013-7944.

[4] R. Eligehausen, G. Sawade, A fracture mechanics based description of the pull-out behavior of headed studs embedded in concrete, Fracture mechanics of concrete structures;, London : Chapman and Hall, 1989, pp. p. 281-299, 0-412-30680-8.

[5] R. Eligehausen, P. Bouska, V. Cervenka, R. Pukl, Size effect of the concrete cone failure load of anchor bolts, In: Bazant Z. (Ed.), Fracture mechanics of concrete structures : FraMCoS1. London, London ed., Elsevier Applied Science,ISBN 1-85166-869-1, 1992, pp. p. 517-525, 1-85166-869-1,.

[6] P. Pivonka, R. Lackner, H. A. Mang, Concrete subjected to triaxial stress states: Application to pull-out analyses, J.Eng.Mech., 130, 12, American Society of Civil Engineers, 2004, pp. 1486-1498, .

[7] R. W. Cannon, E. G. Burdette, R. R. Funk, T. V. Authority, Anchorage to concrete, Tennessee Valley Authority, Division of Engineering Design, Thermal Power Engineering, 1975,.

[8] ACI Committee 349, Code Requirements for Nuclear Safety Related Concrete Structures (ACI 349-90), American Concrete Institute, Farmington Hills, Mich, 1990,.

[9] BSI Committee, DD CEN/TS 1992-4-2:2009, Design of fastenings for use in concrete, Part 4-2: Headed Fasteners, BSI Group, London, 2009,.

[10] R. Cannon, D. Godfrey, F. Moreadith, Guide to the design of anchor bolts and other steel embedments, Concr.Int., 3, 7, 1981, pp. 28-41, .

[11] V. Červenka, L. Jendele, J. Červenka, ATENA Program Document.–Part 1: Theory, Cervenka Consulting, Prague, 2007,.

[12] CEB-FIP, Model Code 1990, First Draft ed., Comitte Euro-International du Beton, Bulletin d´information No. 195,196, Mars, 1990,.

[13] E. Vos, Influence of Loading Rate and Radial Pressure on Bond in Reinforced Concrete.A Numerical and Experimental Approach, Delft University, 1983,.

[14] J. Fornusek, P. Konvalinka, Numerical investigation of head diameter influence on tensile capacity of headed studs, Business, Engineering and Industrial Applications (ISBEIA), 2012 IEEE Symposium, IEEE, 2012, pp. 737-741, .